PAPER • OPEN ACCESS

Structural similarity between dry and wet sphere packings

New Journal of Physics
The open access journal at the forefront of physics

Deutsche Physikalische Gesellschaft DPG
IOP Institute of Physics

Published in partnership with: Deutsche Physikalische Gesellschaft and the Institute of Physics

OPEN ACCESS

RECEIVED
22 January 2019

REVISED
24 March 2019

ACCEPTED FOR PUBLICATION
1 April 2019

PUBLISHED
15 April 2019

PAPER

Structural similarity between dry and wet sphere packings

Simon Weis[1], **Gerd E Schröder-Turk**[1,2,3] **and Matthias Schröter**[4,5]

[1] Institut für Theoretische Physik I, Friedrich-Alexander-Universität Erlangen-Nürnberg, D-91058 Erlangen, Germany
[2] Maths & Stats, School of Engineering and Information Technology, Murdoch University, Perth, Australia
[3] Applied Maths, Research School of Physical Sciences & Engin., Australian National Univ., Canberra, Australia
[4] Institute for Multiscale Simulation, Friedrich-Alexander-Universität Erlangen-Nürnberg, D-91052 Erlangen, Germany
[5] Max Planck Institute for Dyamics and Self-Organization, D-37077 Göttingen, Germany

E-mail: matthias.schroeter@ds.mpg.de

Keywords: wet granular matter, capillary bridges, Minkowski tensors, x-ray tomography, self-assembly

Abstract

The mechanical properties of granular materials change significantly in the presence of a wetting liquid which creates capillary bridges between the particles. This results e.g. in a reduced value of the volume fraction when a packing is prepared with added liquid. Here we use x-ray tomography to demonstrate that this change in mechanical properties is not accompanied by structural differences between dry and wet sphere packings when compared at the same volume fraction. We characterize the structure of the packings by the average numbers of contacts of each sphere $\langle Z \rangle$ and the shape isotropy $\langle \beta_0^{2,0} \rangle$ of the Voronoi cells of the particles. Additionally, we show that the number of liquid bridges per sphere $\langle B \rangle$ is approximately equal to $\langle Z \rangle + 2$, independent of the volume fraction of the packing. These findings will be helpful in guiding the development of both particle-based models and continuum mechanical descriptions of wet granular matter.

1. Introduction

Everyone who has ever built a sand castle at the beach is familiar with the different mechanical properties of wet and dry granular media. Adding a small amount of a wetting liquid to the particles allows the formation of capillary bridges between particles [1–7]. These bridges add tensile forces to the packing, resulting in a significantly increased mechanical stability [8–26]: it is simple to build vertical sand castle walls from wet sand while the same material in its dry state can not form piles with steeper slopes than its angle of repose around 30°, which is dependent on the friction coefficient of the sand.

However, this intuitive notion of additional tensile forces from capillary bridges has not yet been translated into a quantitative theory capable of predicting the properties of a specific wet granular material. Part of the problem is that while x-ray tomography studies [27–30] have provided a more detailed picture of the liquid morphologies inside wet packings, it is still unclear how much these additional tensile forces also lead to geometrical rearrangements of the particles by drawing close-by particles together. Such rearrangements can change the mechanical properties of the sample: The stability of a granular sample is conferred by its force chains [31–35], which consist of lines of contacts. Therefore a change of fabric could modify the mechanical behavior independently of the tensile nature of the bridges.

In this work we demonstrate that while adding liquid to a sphere packing does introduce tensile forces, it does not significantly change the geometrical arrangement of our sphere packings. And due to their disability to interlock when compared to other particle shapes, spheres can be expected to be most susceptible to such geometrical changes.

2. Experiments

2.1. Packing preparation

We prepare wet and dry packings of approximately 5000 monodisperse Polyoxymethylene (POM) spheres (diameter $d = 3.5 \pm 0.022$ mm) in a plexiglass cylinder of 84 mm diameter and 150 mm height. In order to

avoid crystallization [36] in the dry experiments, the container walls are lined with bubble wrap foil. Wet packings are prepared by distributing Bromodecane between the spheres by continuously rotating and shaking the container. The actual formation of liquid bridges due to liquid flow inside a porous matrix is an interesting topic [37–39] which is however beyond the reach of this study.

Bromodecane was chosen because it wets POM surfaces well and provides good x-ray contrast to POM. We will show below that all particles in contact have liquid bridges. We note our earlier failed attempts to use glass particles with a solution of CsCl in water, which did not result in a homogeneous distribution of the liquid. Measurements are performed for liquid volume fractions $\eta = 0\%$, $\eta = 2.1\%$ and $\eta = 3.1\%$, where η is defined as the total liquid volume divided by the total sample volume [11, 27].

In choosing our experimental parameters we need to consider the ratio of gravitational and surface tension forces in our sample, which is measured by the Eötvös number $Eo = \Delta\rho\ g\ d^2/\sigma$ where g is the gravitational acceleration. Inserting our values for the density difference $\Delta\rho = 1.4\ \mathrm{g\ cm^{-3}}$ and surface tension $\sigma = 30\ \mathrm{mN\ m^{-1}}$ we obtain $Eo = 5.7$, i.e. gravitational forces dominate, but surface tension still plays an important role.

The contribution of surface tension to the mechanical stability of the packings becomes evident when comparing the range of accessible global volume fractions ϕ_g: wet packings have a volume fractions after preparation in the range 0.575–0.591[6]. Continuous vertical shaking (30–6000 s, 30 Hz, maximal acceleration 8 g) increases their ϕ_g to only 0.588–0.605. In contrast,we could not prepare dry packings at ϕ_g below 0.61; vertical tapping (10–160 000 sinusoidal taps with a maximal acceleration of 2 g) increases ϕ_g up to 0.64 [40, 41] . These non-overlapping ϕ_g ranges of wet and dry packings are a clear testimonial to the influence of liquid bridges on the mechanical properties, even at a Eötvös number larger one.

2.2. Data acquisition

The internal structure of the packings is evaluated using x-ray tomography; wet samples are measured with a CT-Rex (Fraunhofer EZRT, voxel resolution 35 μm), dry samples with a Nanotom (GE Sensing and Inspection, voxel resolution 64 μm). The image size after cropping the boundary is $1300 \times 1300 \times 1000$ voxels in both setups.

Bromodecane has a vapor pressure of 5.33 Pa at 25 °C [42] which is approximately 600 times smaller than the vapor pressure of water. In consequence all liquid-redistribution inside the packing will happen in surface films and not via the vapor phase. Therefore all wet packings were prepared at least 30 minutes prior to the measurements in order to allow the bromodecane to equilibrate [27, 28].

Particle center positions are detected for all particles, but the further analysis is limited to the $N \approx 800$ particles which are at least 20 mm away from the boundaries, using the methods described in [43][7]. Voxels representing bromodecane are detected by a second binarisation with another, higher threshold. Figure 1 shows cross-sections of the raw and segmented tomographies. Rendered visualizations of the wet packings can be found at [44, 45].

2.3. Computing global volume fractions

The global volume fraction inside our analysis area is the harmonic mean [43, 46] of the local volume fractions ϕ_l^i of the individual particles i inside that area. ϕ_l^i is calculated as the ratio of the volume of particle i and the volume of its Voronoi cell [47–50] i.e. the volume which is closer to this spheres center than to any other sphere center

2.4. Computing contact and bridge numbers

The next step is the determination of the average contact numbers $\langle Z \rangle$ and the average bridge number $\langle B \rangle$, see figure 2. The former describes how many other sphere surfaces a typical particle touches, the latter counts the number of liquid bridges formed by an average particle. $\langle Z \rangle$ is determined using the 'contact number scaling function' method [43, 51–55]; this method uses the ensemble of all interparticle distances to determine the correct threshold distance up to which two particles are considered to be in contact. $\langle B \rangle$ is measured by detecting all liquid domains which connect the surface of two spheres. As expected for a good wetting fluid, for all particle pairs in contact there is also a bridge present at that contact. We also find that within the central region of the packing less than 1% of all liquid domains touch only one particle; and not a single liquid domain involves three touching particles, so called trimers. The latter is expected to change for higher values of η.

[6] It was not feasible to increase ϕ_g in wet packings above 0.605 because longer shaking lead to crystallization of the sample and we could not use rough container boundaries as this would have led to inhomogeneous liquid distributions.

[7] Parameters for image processing: Bilateral filter $\sigma_g = 4$ in units of voxels, $\sigma_p = 2700$ in units of greyvalues and an erosion depth $\lambda = 5$ voxels.

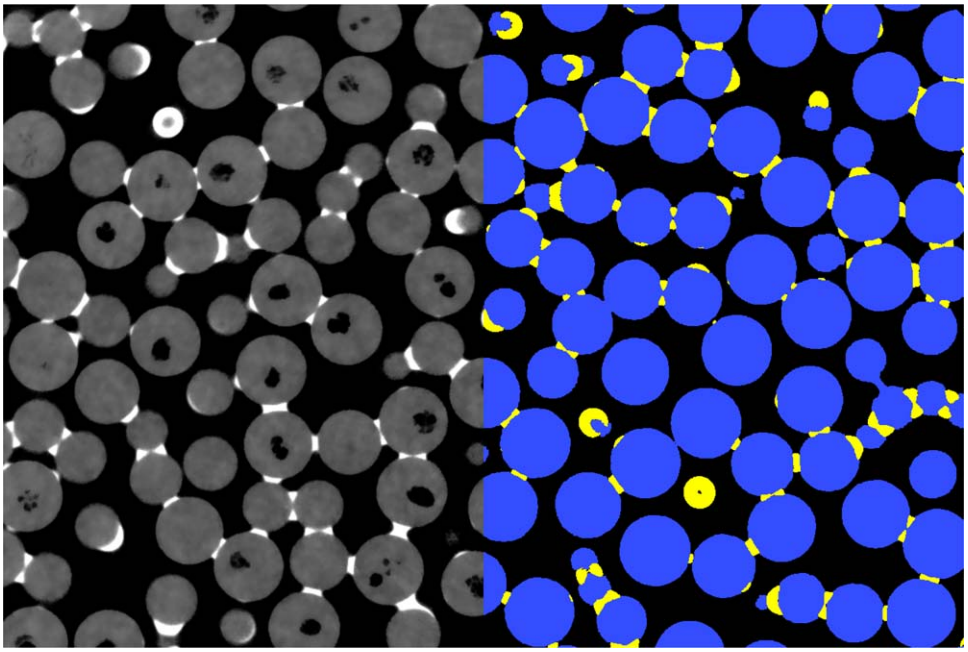

Figure 1. Horizontal slice through a tomogram of a wet packing with a liquid content of 3.1%. *Left*: raw data after applying a bilateral filter for noise reduction. White areas are liquid domains and gray areas particles. Holes inside the particles are due to manufacturing and are removed by image processing. *Right*: after image processing pixels belonging to spheres are marked blue and yellow areas correspond to liquid clusters.

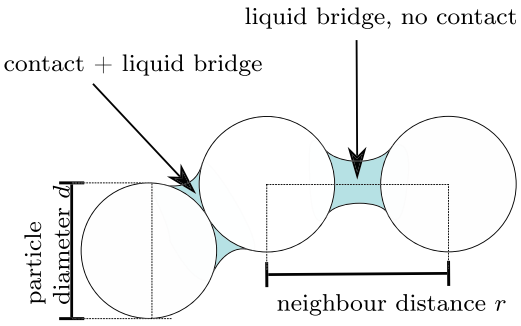

Figure 2. Sketch of the two different types of liquid bridges. In all our experiments, we have found not a single particle contact without an associated liquid bridge.

2.5. Analyzing the shape of the Voronoi cells

Voronoi cell shape analysis is based on a morphometric Minkowski tensor isotropy analysis [56, 57]. Specifically, we calculate the volume moment tensors $\mathbf{W}_0^{2,0}(K) := \int_K \mathbf{r} \otimes \mathbf{r}\, \mathbf{dV}$ of each individual Voronoi cell K where the origin is chosen to be the particle center point, $\mathbf{r}$ is the position vector, and $\otimes$ is the symmetric tensor product. The shape of the Voronoi cell is then characterized by the ratio of the smallest to largest eigenvalue $\beta_0^{2,0} = \frac{\epsilon_{\min}}{\epsilon_{\max}}$ where $\epsilon_{\min}$, $\epsilon_{\max}$ are the smallest and largest eigenvalue, respectively; note that the eigenvalues are positive. When applied to the Voronoi partition, these Minkowski structure metrics have become commonly used structure metrics [58–60], complementary to other metrics such as the two-point correlation function.

3. Comparing wet and dry packings

3.1. Contact and bridge number

Figure 3 summarizes our results for $\langle Z \rangle$ and $\langle B \rangle$. Our main finding here is that, within experimental noise, the average $\langle Z \rangle$ of both wet and dry packings seem to be consistent with the previously published empirical model

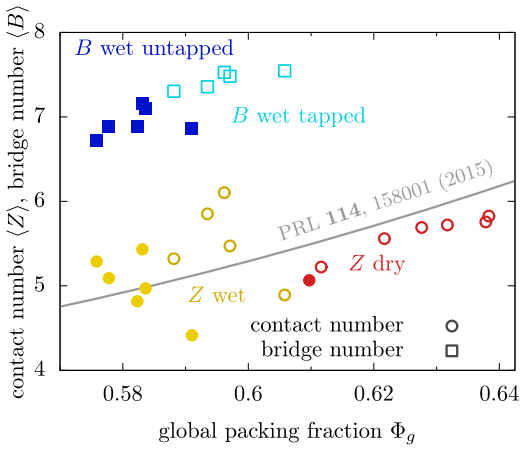

Figure 3. Both bridge number $\langle B\rangle$ and contact number $\langle Z\rangle$ increase with increasing volume fraction. Contact numbers are shown as red (dry) and yellow (wet) circles, bridge numbers as blue and turquois squares. Wet measurements correspond to $\eta = 2.1\%$. Open and closed symbols correspond to tapped and untapped system preparation, respectively.

for dry spheres [55]. The small but systematic deviations of the dry packing data from the model can be explained by the larger asphericity of the 3D printed particles used in [55]. For more details see appendix B.

It is also noteworthy that the $\langle Z\rangle$ values of wet packings fluctuate more strongly from preparation to preparation than those of dry packings, in contrast to the $\langle B\rangle$ values which display a smoother increase with ϕ_g. Dry packings are hyperstatic, i.e. the contact forces provide more constraints than what is needed to fix all the degrees of freedom of the particles [61]. In absense of a dominating mechanical constraint, the dependence of $\langle Z\rangle$ on ϕ_g originates from geometrical effects such as volume exclusion [62, 63]. In wet packings, hyperstaticity is even stronger than in dry packings due to the addition of the capillary bridges as another force transmission mechanism. However, the stronger fluctuations of $\langle Z\rangle$ compared to $\langle B\rangle$ indicates that the physics of wet packings might be less determined by volume exclusion (which is strongly connected to ϕ_g) than by the preparation dependent interplay between tensile and compressive forces.

Figure 3 shows also that in wet packings each particle has on average two liquid bridges that do not correspond to a particle contact: $\langle B\rangle - \langle Z\rangle \approx 2$ (keeping in mind that each contact also corresponds to a liquid bridge). Put differently, the number of force transmission channels for compressive forces (at the contact points) is by two lower than the number of force transmission points for tensile, cohesive forces (all liquid bridges).

We note that our results on the relationship between $\langle Z\rangle$ and $\langle B\rangle$ could also be helpful to extend statistical mechanics approaches to unsaturated porous media [64].

3.2. Voronoi cell shape

The Voronoi cell shape analysis shown in figure 4 reinforces the conclusion that wet packings can be thought of as dry packings with additional liquid bridges introduced between particles that are not in contact but very close by. It shows the average isotropy index over all particles $\langle\beta_0^{2,0}\rangle$, calculated for all dry and wet packings. The average packing isotropy $\langle\beta_0^{2,0}\rangle$ allows for no identification of a structural difference between dry and wet packings. Both wet and dry systems coincide with earlier independent results [58]. For the system and length scale studied here, this supports the conclusion that, structurally, the wet packings are 'just dry packings with added liquid bridges', with the presence of the liquid bridges not being accompanied by a significant change in structure of the packing.

Another commonly used metric to study the structure of amorphous packings is the pair correlation function. We show in the appendix that there are again no differences between wet and dry packings within the experimental resolution of our data.

4. Probability of a liquid bridge forming between spheres

While both $\langle Z\rangle$ and $\langle B\rangle$ depend on ϕ_g, the fraction $\zeta(r)$ of particle pairs at distance r that are connected through a liquid bridge (called *bridge probability*) does not. This is shown in figure 5 using a rescaled distance r' between particles: $r' = (r - d)/d$. Particles in contact always have a liquid bridge, $\zeta(0) = 1$, as expected for a good wetting liquid. Liquid bridges between particle pairs with gap distances $r - d > 0.15d$ do not occur within our packings. Between these two limits, $\zeta(r)$ decays monotonously with a slope that is independent of ϕ_g.

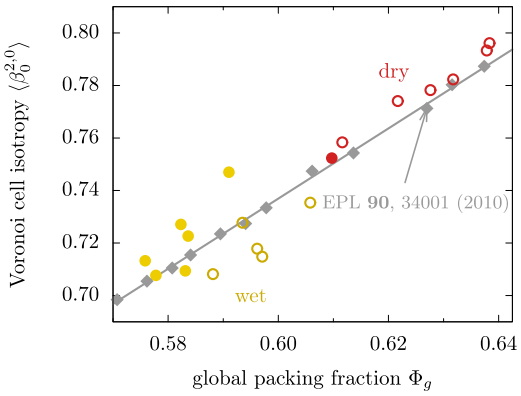

Figure 4. Adding liquid to a packing does not change the shape of the Voronoi cells: the average cell isotropy $\langle\beta_0^{2,0}\rangle$ of dry (red circles) and wet (yellow circles) packings agrees with the previously published data (gray diamonds) for dry sphere packings [58]. Open and closed symbols correspond to figure 3.

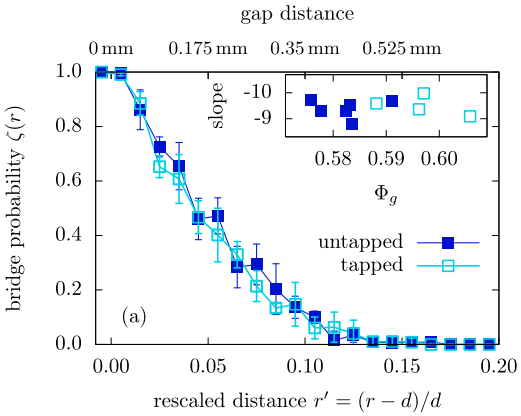

Figure 5. The probability ζ that a liquid bridge exists between two particles depends only on their distance r, not the global volume fraction ϕ_g of the packing. Here the distance between spheres is rescaled with the particle diameter d: $r' = (r - d)/d$. Typical liquid bridges between particles extend up to $0.15d$. To improve statistics, we have averaged all tapped and all untapped experiments. The inset provides the proof that this is permissible because $\zeta(r')$ does not depend on ϕ_g: the slope of the curves, determined from a linear fit to $\zeta(r')$ in the range between 0 and 0.1, is constant for all experiments.

This result supports an inversion of our main argument: while the geometry of the packing does change (increasing ϕ_g does change the pair correlation function), the probability of formation of liquid bridges seems to be unaltered (which points to liquid properties such as surface tension as the main control parameter).

All data for wet packings shown in figures 3–5 are for a liquid volume fraction $\eta = 2.1\%$. Figure 6 addresses the natural question how the shape and distributions of liquid bridges changes when the liquid volume fraction is increased: the main effect is an increase in the volume (and hence shape) of the liquid bridges, not the creation of additional longer liquid bridges.

Figure 6(a) shows that while the bridge probability $\zeta(r)$ does increase slightly for $\eta = 3.1\%$, there is no emergence of longer bridges: $\zeta(r)$ still drops to zero for $r - d \approx 0.016d$. The main effect of increasing η is a proportional increase in size of the liquid bridges: within statistical accuracy the ratio of the average bridge volumes $\langle V_B\rangle$ at $\eta = 2.1\%$ and $\eta = 3.1\%$ corresponds to the ratio of added bromodecane for all values of r'. It is a worthwhile future question beyond the scope of this article to investigate in more detail the shape and volume of the liquid bridges (considering the resolution of our CT data, details of the shape can be probed; a volume of $200nL$ corresponds to approximately 4000 voxels).

5. Conclusion

We have found that the structure of the wet packings to be very similar to that of a dry packing at the same packing fraction. This is a surprising result considering that the presence of the wetting liquid has a clear

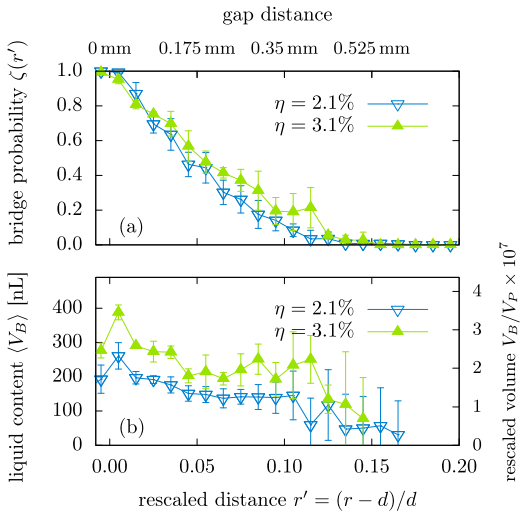

Figure 6. Adding more liquid increases the number of and the average volume inside liquid bridges. But it does not create additional bridges between particles that are further apart. This is shown in panel (a) typical liquid bridges extend up to 0.15 particle diameters regardless if the liquid content η is 2.1% or 3.1%. (b) The average volume inside liquid clusters $\langle V_B \rangle (r')$ increases with η. If no liquid bridges exist in a given distance bin, the corresponding data point is omitted. Data is averaged over 11 ($\eta = 2.1\%$) respectively 7 ($\eta = 3.1\%$) experiments.

influence on the mechanical properties. Our conclusions depend almost certainly on the sphere diameter because the relative importance of surface tension forces compared to gravitational forces increase when d decreases. Our results are for beads of diameter 3.5 mm where liquid bridges are relevant for the mechanical properties, despite not affecting the structure of the bead pack. Future research should explore the limit of smaller particles, where the presence of a wetting liquid can stabilize packings at substantially lower packing fractions than what can be reached in dry packings. A second important avenue for future research will be non-spherical particles which introduce not only new liquid bridge geometries but also interesting new geometrical features in dry packings.

Acknowledgments

We are grateful to Martin Brinkmann (Saarbrücken) for advice and discussion, and Klaus Mecke and Thorsten Pöschel (both Erlangen) and Stephan Herminghaus (Göttingen) for support. We acknowledge funding by the German Science Foundation (DFG) under grant SCHR-1148/3-2 within the research group 'Geometry and Physics of Spatial Random Systems' and through the Cluster of Excellence 'Engineering of Advanced Materials'. GEST acknowledges support through a collaboration scheme of Universities Australia and the German Academic Exchange Service (DAAD).

Appendix A. Comparing $g(r)$ of dry and wet packings

The pair correlation function $g(r)$ is a commonly used structural measure for granular packings. It is known that the features of the pair correlation function $g(r)$ of granular packings depend on the global packing fraction Φ_g of the packing. Packing fractions for wet and dry packings did not overlap in our experiments. Therefore we show the packings with the smallest difference in global packing fraction, when comparing the pair correlation function $g(r)$ for wet and dry packings in figure A1. The wet packing has a value of $\Phi_g = 0.6058$ and the dry packing of $\Phi_g = 0.6097$. As it can be seen in figure A1 no structural differences are revealed by $g(r)$

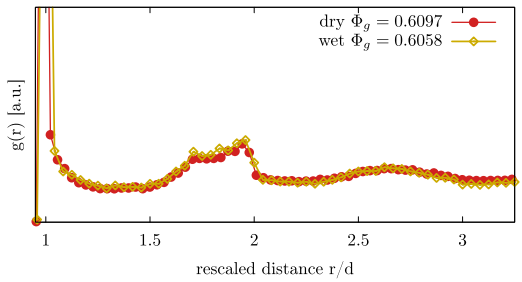

Figure A1. Within the statistics of our measurement no structural differences are revealed by $g(r)$. Pair correlation function $g(r)$ comparison between a wet packing at $\Phi_g = 0.6058$ and a dry packing at $\Phi_g = 0.6097$.

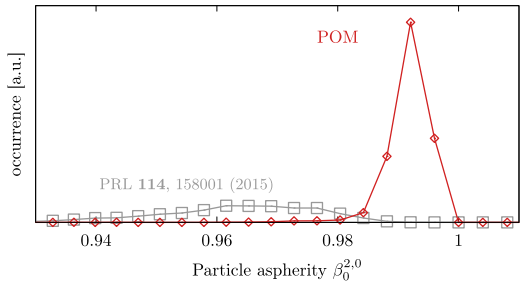

Figure B1. The particle asphericity distribution for the particles used in this work (POM) is significantly closer to one than for the 3D printed particles used in [55].

Appendix B. Comparing the particles in this work and in Schaller *et al Phys. Rev. Lett.* 2015 114 158001

As shown in figure B1, the 3D printed particles used in Schaller *et al Phys. Rev. Lett.* 2015 **114** 158001 [55] are characterized by an average asphericity $\beta_0^{2,0}$ (the asphericity is evaluated on the particle shape, not its Voronoi cell) of 0.96 ± 0.01 whereas the particles used here are more spherical with $\beta_0^{2,0} \approx 0.992 \pm 0.004$. It is known that with increasing particle asphericity (decreasing particle aspect ratio) the average contact number $\langle Z \rangle$ increases. This explains the deviations in the contact number between the particles used in this article and in Schaller *et al Phys. Rev. Lett.* 2015 **114** 158001.

References

[1] Hornbaker D, Albert R, Albert I, Barabási A L and Schiffer P 1997 *Nature* **387** 765
[2] Halsey T C and Levine A J 1997 *Phys. Rev. Lett.* **80** 3141–4
[3] Mason T G, Levine A J, Ertaş D and Halsey T C 1999 *Phys. Rev.* E **60** R5044–7
[4] Kohonen M M, Geromichalos D, Scheel M, Schier C and Herminghaus S 2004 *Physica* A **339** 7–15
[5] Butt H J and Kappl M 2009 *Adv. Colloid Interface Sci.* **146** 48–60
[6] Gögelein C, Brinkmann M, Schröter M and Herminghaus S 2010 *Langmuir* **26** 17184–9
[7] Herminghaus S 2013 *Wet Granular Matter: A Truly Complex Fluid* (Singapore: World Scientific)
[8] Mason G and Clark W 1968 *Nature* **219** 149–50
[9] Pierrat P and Caram H S 1997 *Powder Technol.* **91** 83–93
[10] Tegzes P, Vicsek T and Schiffer P 2002 *Phys. Rev. Lett.* **89** 094301
[11] Scheel M, Geromichalos D and Herminghaus S 2004 *J. Phys.: Condens. Matter* **16** S4213–8
[12] Fournier Z *et al* 2005 *J. Phys.: Condens. Matter* **17** S477–502
[13] Huang N, Ovarlez G, Bertrand F, Rodts S, Coussot P and Bonn D 2005 *Phys. Rev. Lett.* **94** 028301
[14] Richefeu V, El Youssoufi M S and Radjaï F 2006 *Phys. Rev.* E **73** 051304
[15] Xu Q, Orpe A V and Kudrolli A 2007 *Phys. Rev.* E **76** 031302
[16] Møller P C F and Bonn D 2007 *Europhys. Lett.* **80** 38002
[17] Huang K, Sohaili M, Schröter M and Herminghaus S 2009 *Phys. Rev.* E **79** 010301
[18] Rahbari S H E, Vollmer J, Herminghaus S, Brinkmann M and Rahbari E 2009 *Europhys. Lett.* **87** 14002
[19] Fiscina J E, Lumay G, Ludewig F and Vandewalle N 2010 *Phys. Rev. Lett.* **105** 048001
[20] Liu P Y, Yang R Y and Yu A B 2011 *Phys. Fluids* **23** 013304
[21] Vandewalle N, Lumay G, Ludewig F and Fiscina J E 2012 *Phys. Rev.* E **85** 031309
[22] Fiscina J E, Pakpour M, Fall A, Vandewalle N, Wagner C and Bonn D 2012 *Phys. Rev.* E **86** 020103
[23] Fall A, Weber B, Pakpour M, Lenoir N, Shahidzadeh N, Fiscina J, Wagner C and Bonn D 2014 *Phys. Rev. Lett.* **112** 175502
[24] Bossler F and Koos E 2016 *Langmuir* **32** 1489–501

[25] Kovalcinova L, Karmakar S, Schaber M, Schuhmacher A L, Scheel M, DiMichiel M, Brinkmann M, Seemann R and Kondic L 2018 *Phys. Rev.* E **98** 032905
[26] Liefferink R W, Weber B and Bonn D 2018 *Phys. Rev.* E **98** 052903
[27] Scheel M, Seemann R, Brinkmann M, Di Michiel M, Sheppard A, Breidenbach B and Herminghaus S 2008 *Nat. Mater.* **7** 189–93
[28] Scheel M 2009 Experimental investigations of the mechanical properties of wet granular matter *PhD Thesis* University of Göttingen http://hdl.handle.net/11858/00-1735-0000-0006-B4BC-4
[29] Mani R, Semprebon C, Kadau D, Herrmann H J, Brinkmann M and Herminghaus S 2015 *Phys. Rev.* E **91** 042204
[30] Saingier G, Sauret A and Jop P 2017 *Phys. Rev. Lett.* **118** 208001
[31] Majmudar T S and Behringer R P 2005 *Nature* **435** 1079–82
[32] Puckett J G and Daniels K E 2013 *Phys. Rev. Lett.* **110** 058001
[33] Brodu N, Dijksman J A and Behringer R P 2015 *Nat. Commun.* **6** 6361
[34] Daniels K E, Kollmer J E and Puckett J G 2017 *Rev. Sci. Instrum.* **88** 051808
[35] Kollmer J E and Daniels K E 2019 *Soft Matter* **15** 1793–8
[36] Hanifpour M, Francois N, Robins V, Kingston A, Vaez Allaei S M and Saadatfar M 2015 *Phys. Rev.* E **91** 062202
[37] Lenormand R, Zarcone C and Sarr A 1983 *J. Fluid Mech.* **135** 337–53
[38] Lenormand R, Touboul E and Zarcone C 1988 *J. Fluid Mech.* **189** 165–87
[39] Lenormand R and Zarcone C 1989 *Transp. Porous Media* **4** 599–612
[40] Knight J B, Fandrich C G, Lau C N, Jaeger H M and Nagel S R 1995 *Phys. Rev.* E **51** 3957–63
[41] Ribière P, Richard P, Bideau D and Delannay R 2005 *Eur. Phys. J.* E **16** 415–20
[42] Mackay D, Shiu W Y, Ma K C and Lee S C 2006 *Handbook of Physical-Chemical Properties and Environmental Fate for Organic Chemicals* (Boca Raton, FL: CRC Press)
[43] Weis S and Schröter M 2017 *Rev. Sci. Instrum.* **88** 051809
[44] Rendering of a slice of liquid clusters in the packing: https://youtube.com/watch?v=ut2CuAqNcKM
[45] Rendering of one particle with all liquid bridges connected to this particle and the respective other particles https://youtu.be/PaJxVjaGURY
[46] Aste T 2006 *Phys. Rev. Lett.* **96** 018002
[47] Voronoi G 1909 *J. Reine Angew. Math.* **136** 67
[48] Rycroft C H 2009 *Chaos* **19** 041111
[49] Weis S, Schönhöfer P W A, Schaller F M, Schröter M and Schröder-Turk G E 2017 *EPJ Web Conf.* **140** 06007
[50] Institute of Theoretical Physics Pomelo 2018 http://theorie1.physik.fau.de/research/pomelo/index.html
[51] Rintoul M D and Torquato S 1998 *Phys. Rev.* E **58** 532–7
[52] Aste T, Saadatfar M and Senden T 2005 *Phys. Rev.* E **71** 061302
[53] Aste T, Saadatfar M and Senden T J 2006 *J. Stat. Mech.* 07010
[54] Schaller F M, Neudecker M, Saadatfar M, Delaney G, Mecke K, Schröder-Turk G E and Schröter M 2013 *AIP Conf. Proc.* **1542** 377
[55] Schaller F M, Neudecker M, Saadatfar M, Delaney G W, Schröder-Turk G E and Schröter M 2015 *Phys. Rev. Lett.* **114** 158001
[56] Schröder-Turk G *et al* 2011 *Adv. Mater.* **23** 2535–53
[57] Schröder-Turk G, Mickel W, Kapfer S, Schaller F, Breidenbach B, Hug D and Mecke K 2013 *New J. Phys.* **15** 083028
[58] Schröder-Turk G, Mickel W, Schröter M, Delaney G, Saadatfar M, Senden T, Mecke K and Aste T 2010 *Europhys. Lett.* **90** 34001
[59] Kapfer S, Mickel W, Mecke K and Schröder-Turk G 2012 *Phys. Rev.* E **85** 030301(R)
[60] Schaller F M *et al* 2015 *Europhys. Lett.* **111** 24002
[61] Schröter M 2017 *EPJ Web Conf.* **140** 01008
[62] Song C, Wang P and Makse H A 2008 *Nature* **453** 629–32
[63] Baule A, Mari R, Bo L, Portal L and Makse H A 2013 *Nat. Commun.* **4** 2194
[64] Xu J and Louge M Y 2015 *Phys. Rev.* E **92** 062405